

## Metal-insulator transition in the double perovskites

A. A. Aligia, P. Petrone, J. O. Sofo, and B. Alascio

*Comisión Nacional de Energía Atómica, Centro Atómico Bariloche and Instituto Balseiro, 8400 S.C. de Bariloche, Argentina*

(Received 18 September 2000; revised manuscript received 17 May 2001; published 15 August 2001)

We construct an effective Hamiltonian for the motion of electrons among the transition-metal ions of ordered double perovskites like  $\text{Sr}_2\text{FeMoO}_6$ , in which strong intra-atomic Coulomb repulsion  $U$  is present in only one of the inequivalent transition metal sites. Using a slave-boson formalism, we construct a phase diagram that describes a charge-transfer transition between insulating and metallic behavior as the parameters of the model are changed. The parameters for  $\text{Sr}_2\text{FeMoO}_6$  are estimated from first-principles calculations and a transition to the insulating state with negative pressure is obtained.

DOI: 10.1103/PhysRevB.64.092414

PACS number(s): 75.30.Vn, 71.30.+h

Two mechanisms contribute to the magnetoresistance (MR) of Mn Perovskites. One of them is an intrinsic mechanism that results from the quenching of spin scattering of the carriers by localized spins. It dominates the high-field MR and is most effective at temperatures of the order of the Curie temperature  $T_c$ . The other mechanism, which is most effective at low fields, is due to the lowering of spin scattering at interphases between two regions in the materials that have different orientations of their magnetization. This mechanism is also temperature dependent and is larger at temperatures well below  $T_c$ , where the polarization of carriers is large. This explains the interest on materials where  $T_c$  is appreciably larger than room temperature.

The report by Kobayashi *et al.*<sup>1</sup> that the double perovskite  $\text{Sr}_2\text{FeMoO}_6$  with a  $T_c$  of about 450 K is half metallic with an appreciable low-field magnetoresistance has renewed interest in these compounds. Furthermore, they open new questions concerning the nature of the electronic structure.

In an ionic picture, assuming that all O ions are  $\text{O}^{2-}$ , one can imagine the 3d transition-metal ions as triply or doubly ionized, and Mo to be  $\text{Mo}^{5+}(4d^1, S=1/2)$  or  $\text{Mo}^{6+}(4d^0, S=0)$ . In this picture  $\text{Fe}^{3+}(3d^5, S=5/2)$  would order antiferromagnetically with Mo to produce a magnetization saturation of  $4\mu_B$  as observed, or  $\text{Fe}^{2+}(3d^6, S=2)$  could order ferromagnetically to produce the same magnetization. In the extreme situation with no carriers on the Mo ion ( $\text{Fe}^{2+}$  and  $\text{Mo}^{6+}$ ), one would expect that the system is insulating because of the strong intra-atomic Coulomb repulsion in Fe [ $U \sim 7$  eV (Ref. 2)] compared with the effective Mo-Fe hopping [ $V \sim 0.39$  eV from our fits explained below or  $V \sim 0.25$  eV (Ref. 3)]. Actually, there is a certain degree of covalency between O and the transition-metal ions.<sup>4</sup> Applying perturbation theory to this insulating state, the Mo valence becomes  $v_{\text{Mo}} = 6 - 24[t_{\text{Mo-O}}/(\epsilon_{\text{Mo}} - \epsilon_{\text{O}})]^2$ , where  $t_{\text{M-O}}$  is the hopping between transition-metal  $t_{2g}$  and O  $p_\pi$  orbitals,<sup>5</sup> and  $\epsilon_X$  is the on-site energy for atom X. The magnetic moment of Mo,  $\mu_{\text{Mo}}$ , remains zero in second order in  $t_{\text{M-O}}$ . This shows that  $\mu_{\text{Mo}}$  rather than  $v_{\text{Mo}}$  can indicate if the system is insulating or near a metal-insulator transition. In fact, the observed Mo-3d chemical shift is practically identical to that of  $\text{MoO}_3$ , but  $v_{\text{Mo}} < 6$ .<sup>4</sup> For Fe,  $v_{\text{Fe}} - 2 = 4 - \mu_{\text{Fe}} = 8[t_{\text{Fe-O}}/(\epsilon_{\text{Fe}} - \epsilon_{\text{O}})]^2$ .

While  $\text{Sr}_2\text{FeMoO}_6$  is in fact metallic, neutron-diffraction experiments<sup>6</sup> obtained magnetic moments consistent with an

insulating state:  $\mu_{\text{Mo}} = 0 \pm 0.1 \mu_B$  and  $\mu_{\text{Fe}} = 4 \pm 0.1 \mu_B$ , indicating that the system is near a metal-insulator transition. Our band-structure calculations give a metallic state with  $\mu_{\text{Mo}} \approx 0.2 \mu_B$ , and with a sign opposite to that of  $\mu_{\text{Fe}}$ . The fact that the experimental  $\mu_{\text{Mo}}$  is lower, points out that the real system is nearer to the insulating state than the predictions of these calculations. Furthermore, substitution of Mo by Re seems to increase  $T_c$  but renders the material insulating.<sup>7</sup> In addition, substitution of Fe by Co or Mn, for example, makes the compounds antiferromagnetic and insulating.<sup>8</sup> Also, the physical properties (conductivity, magnetization) are very sensitive to sample preparation. Thus, it is of great interest to understand when we can expect a metallic or insulating behavior in similar systems.

In this paper, we intend to address the general question of when one should expect insulating or metallic behavior in the ordered double-perovskites structures.

In order to investigate the physical properties of these materials it is necessary to gain knowledge of their intimate electronic structure, including the effects of correlations. We build a tight-binding Hamiltonian to describe their electronic structure. This Hamiltonian is based on the calculated energy bands, as explained later, and is reduced to the minimum set of relevant parameters. Since the low-energy properties of the compounds are determined by the bands crossing the Fermi energy, the only interesting orbitals are the  $t_{2g}$  orbitals in the interpenetrating simple-cubic lattices of Fe and Mo. Itinerant electrons tunnel from the three  $t_{2g}$  orbitals of Fe to the same  $t_{2g}$  orbitals of the nearest-neighbor Mo, and between Mo with transfer energies  $V$  and  $V'$ . In the ferromagnetic phase, which will be studied here, only spin-down electrons can jump since the spin-up orbitals at each Fe site are already filled. We consider these orbitals to be frozen. The same approach has been followed in a recent paper.<sup>3</sup> The resulting effective Hamiltonian, which contains strong correlations, is treated in a slave-boson approximation.<sup>9,10</sup>

For our band-structure calculations we use the full-potential linearized-augmented-plane-wave method (FP-LAPW).<sup>11</sup> In brief, this is an implementation of the density-functional theory using the generalized-gradient approximation of the exchange and correlation potential.<sup>13</sup> The Kohn-Sham equations are solved using a basis of linearized augmented plane waves.<sup>12</sup> Local-orbital extensions to the LAPW basis<sup>14</sup> are used to describe the 3s and 3p orbitals of

Fe and the  $4s$  orbitals of Mo and Sr. We use a well-converged basis set of around 1260 plane waves and a sampling of the Brillouin zone of 343 points, corresponding to 20 in the irreducible wedge of the Brillouin-zone. We use a muffin-tin radius of 2.2 Bohrs for Fe, 2.0 Bohrs for Mo, 2.3 Bohrs for Sr and Mo, and 1.5 Bohrs for O.

To construct an effective Hamiltonian for the description of the motion of electrons among transition-metal ions, we consider a simple-cubic lattice occupied by these ions of lattice parameter  $a$ . This lattice consists of two interpenetrating fcc sublattices, one occupied by the Mo ions and the other by the Fe ions, in such a way that the nearest neighbors (NN) of each Mo ion lie in the other sublattice and vice versa. This may be extended to other transition metals. In between each two transition-metal ions lies an O ion. The O degrees of freedom can be eliminated through a low-energy reduction process (see, for example, Refs. 5 and 15 and references therein). If the difference between on-site energies  $\epsilon_{\text{Mo}} - \epsilon_{\text{O}}$  and  $\epsilon_{\text{Fe}} - \epsilon_{\text{O}}$  is large compared with the absolute value of  $t_{\text{Mo-O}}$  and  $t_{\text{Fe-O}}$ , this can be done by perturbation theory. The  $xy$  orbitals acquire an effective hopping  $V$  to the  $xy$  orbitals of the four NN in the  $x$ - $y$  plane due to a process of second order in the hopping between  $xy$  and  $p_{\pi}$  orbitals.<sup>5</sup> There are two third-order processes, which involve O-O hopping between two  $p_{\pi}$  orbitals, which lead to a next-NN hopping  $V'$  between Mo sites. The band calculations suggest that the equivalent process between Fe ions is not important and we neglect it. By symmetry, it is clear that the  $xy$  orbitals cannot hop to NN or next-NN  $yz$  or  $zx$  orbitals. In addition (excluding direct hopping involving  $d$  orbitals at distances larger than  $a/2$ ), the  $xy$  orbitals at any site  $i$  cannot hop out of the plane, because its hopping to any O orbital of the sites  $i \pm (a/2)\hat{\mathbf{z}}$  is also zero by symmetry. Thus, with a high degree of accuracy, electrons occupying  $xy$  orbitals move only in the  $x$ - $y$  plane. Similar considerations extend to the  $yz$  and  $zx$  orbitals.

This leads to the following effective Hamiltonian for the movement of electrons with spin down among  $d$  orbitals:

$$H = E_{\text{Fe}} \sum_{i\alpha} n_{i\alpha} + E_{\text{Mo}} \sum_{j\alpha} n_{j\alpha} + U \sum_{i,\alpha < \beta} n_{i\alpha} n_{i\beta} - V \sum_{i\alpha} (c_{i+\delta_{\alpha}}^{\dagger} c_{i\alpha} + \text{H.c.}) - V' \sum_{j\alpha\gamma_{\alpha}} c_{j+\gamma_{\alpha}}^{\dagger} c_{j\alpha}. \quad (1)$$

Here  $c_{i\alpha}^{\dagger}$  creates an electron at the orbital  $\alpha = xy, yz,$  or  $zx$  of site  $i$  with spin down, the sum over  $i$  ( $j$ ) extends over the Fe (Mo) sites,  $n_{i\alpha} = c_{i\alpha}^{\dagger} c_{i\alpha}$ , and  $\delta_{\alpha}$  ( $\gamma_{\alpha}$ ) are vectors that connect a site with their four NN (next-NN) sites lying in the  $\alpha$  plane.  $U$  is the on-site Coulomb repulsion at the Fe sites. The corresponding term at the Mo sites is neglected. Eliminating the  $d$ - $p_{\pi}$  hopping through a canonical transformation, the values of the other parameters are

$$E_{\text{Fe}} = \epsilon_{\text{Fe}} - \frac{4t_{\text{Fe-O}}^2}{\epsilon_{\text{Fe}} - \epsilon_{\text{O}}}, \quad E_{\text{Mo}} = \epsilon_{\text{Mo}} - \frac{4t_{\text{Mo-O}}^2}{\epsilon_{\text{Mo}} - \epsilon_{\text{O}}},$$

$$V = \frac{t_{\text{Fe-O}} t_{\text{Mo-O}}}{2} \left( \frac{1}{\epsilon_{\text{Fe}} - \epsilon_{\text{O}}} + \frac{1}{\epsilon_{\text{Mo}} - \epsilon_{\text{O}}} \right), \quad (2)$$

$$V' = \frac{2t_{\text{Mo-O}}^2 t_{\text{O-O}}}{(\epsilon_{\text{Mo}} - \epsilon_{\text{O}})^2},$$

where  $t_{\text{O-O}}$  is the absolute value of the hopping between the  $p_{\pi}$  orbitals of two nearest-neighbor O atoms.

In order to treat the Hamiltonian Eq. (1), we use a simple extension of the slave-boson theory of Kotliar and Ruckenstein<sup>9</sup> to the case in which there are two sites per elementary cell and three ‘‘colors’’ per Fe site (instead of two representing spin up and down). The Fock space at each Fe site  $i$  is enlarged introducing boson states represented by the creation operators  $e_i$  (empty),  $s_{i\alpha}$  (singly occupied at orbital  $\alpha$ ),  $d_{i\alpha\beta} = d_{i\beta\alpha}$  (doubly occupied at orbitals  $\alpha$  and  $\beta \neq \alpha$ ), and  $t_i$  (triply occupied). In the combined space  $H$  reads

$$H = E_{\text{Fe}} \sum_{i\alpha} n_{i\alpha} + E_{\text{Mo}} \sum_{j\alpha} n_{j\alpha} + U \sum_i \left( \sum_{\alpha < \beta} d_{i\alpha\beta}^{\dagger} d_{i\alpha\beta} + 3t_i \right) - V \sum_{i\alpha\delta_{\alpha}} (c_{i+\delta_{\alpha}}^{\dagger} c_{i\alpha} z_{i\alpha} + \text{H.c.}) - V' \sum_{j\alpha\gamma_{\alpha}} c_{j+\gamma_{\alpha}}^{\dagger} c_{j\alpha} + \sum_{i\alpha} \lambda_{i\alpha} \left( s_{i\alpha}^{\dagger} s_{i\alpha} + \sum_{\beta \neq \alpha} d_{i\alpha\beta}^{\dagger} d_{i\alpha\beta} + t_i^{\dagger} t_i - n_{i\alpha} \right) + \sum_i \lambda'_i \left( e_i^{\dagger} e_i + t_i^{\dagger} t_i + \sum_{\alpha} s_{i\alpha}^{\dagger} s_{i\alpha} + \sum_{\alpha < \beta} d_{i\alpha\beta}^{\dagger} d_{i\alpha\beta} - 1 \right), \quad (3)$$

where  $z_{i\alpha}^{\dagger}$  represent creation of an electron in the bosonic part of the Fock space,

$$z_{i\alpha}^{\dagger} = \left( 1 - e_i^{\dagger} e_i - \sum_{\beta \neq \alpha} s_{i\beta}^{\dagger} s_{i\beta} - d_{i\gamma\eta}^{\dagger} d_{i\gamma\eta} \right)^{-1/2} \times \left( s_{i\alpha}^{\dagger} e_i + \sum_{\beta \neq \alpha} d_{i\alpha\beta}^{\dagger} s_{i\beta} + t_i^{\dagger} d_{i\gamma\eta} \right) \times \left( 1 - s_{i\alpha}^{\dagger} s_{i\alpha} - \sum_{\beta \neq \alpha} d_{i\alpha\beta}^{\dagger} d_{i\alpha\beta} - t_i^{\dagger} t_i \right)^{-1/2}, \quad (4)$$

where  $\gamma$  and  $\eta$  are the two orbitals different from  $\alpha$ , and the last two terms of Eq. (3) were introduced to satisfy the constraints of vanishing of the corresponding expressions between brackets when the energy is minimized with respect to the Lagrange multipliers  $\lambda_{i\alpha}$  and  $\lambda'_i$ . The roots in Eq. (4) were carefully chosen to satisfy three requirements: (i) they are equal to 1 when treated exactly inside this expression, (ii) they respect electron-hole symmetry, and (iii) when  $U=0$ , the saddle point of Eq. (3) reproduces the exact ground-state energy.

In the following we consider the Hamiltonian (3) in the saddle-point approximation, looking at the homogeneous symmetric solution of the minimization problem, in which all values of the condensed bosons are independent of site and orbital. The problem reduces to a noninteracting one

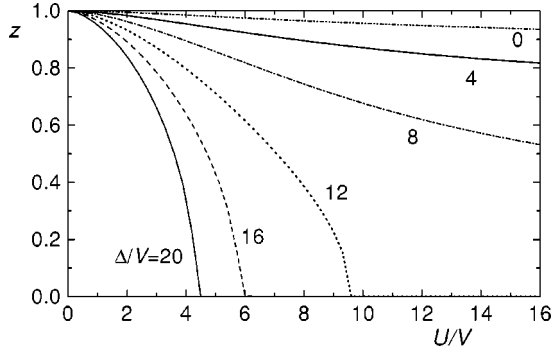


FIG. 1. Reduction factor of the effective hopping as a function of  $U$  for several values of  $\Delta = E_{\text{Mo}} - E_{\text{Fe}}$ .

with renormalized NN hopping  $Vz$ , where  $z$  is the saddle-point value of  $z_{i\alpha}^\dagger$  (assumed real). We neglect the term in  $V'$ . Its effect near the metal-insulator transition is small and can be taken into account renormalizing  $V$ . Taking  $V' = 0$  allows us to obtain analytical expressions for the electronic spectral densities of states  $\rho_{\alpha\text{Fe}}$  and  $\rho_{\alpha\text{Mo}}$  as a function of the saddle-point values of the bosons ( $e$ ,  $s$ ,  $d$ , and  $t$ ) and multiplier  $\lambda_{i\alpha} = \lambda$ ,

$$\rho_{\alpha\text{Fe}}(\omega) = (\omega - E_{\text{Mo}})F(\omega), \quad \rho_{\alpha\text{Mo}}(\omega) = (\omega - E'_{\text{Fe}})F(\omega)$$

with

$$E'_{\text{Fe}} = E_{\text{Fe}} - \lambda, \quad F(\omega) = \rho_0(r)/r,$$

$$r = \text{sgn}(2\omega - E_{\text{Mo}} - E'_{\text{Fe}}) \sqrt{(\omega - E_{\text{Mo}})(\omega - E'_{\text{Fe}})}, \quad (5)$$

and  $\rho_0(\omega)$  is the spectral density for a square lattice with NN hopping  $Vz$ . For simplicity, we replace this density by a constant  $\rho_0 = 1/(2W)$  extending from  $-W$  to  $W$  with  $W = 4Vz$ . This allows to perform the integrals analytically and the energy per Fe site takes the form

$$\begin{aligned} E(s, d, t) = & \frac{E_{\text{Mo}} + E_{\text{Fe}}}{2} - \frac{3[W^2 + (E_{\text{Mo}} - E'_{\text{Fe}})^2/4]^{1/2}}{2} \\ & + [4W^2/9 + (E_{\text{Mo}} - E'_{\text{Fe}})^2/4]^{1/2} \\ & + \frac{1}{4}(1 - 6m)(E_{\text{Mo}} - E_{\text{Fe}} - \lambda) + 3U(d^2 + t^2), \end{aligned} \quad (6)$$

where  $e$  is eliminated using the constraint  $1 = e^2 + t^2 + 3(s^2 + d^2)$ ,  $m = s^2 + 2d^2 + t^2$ , and  $\lambda$  is eliminated from

$$\begin{aligned} \langle n_{i\alpha} \rangle = m = & \frac{1}{6} + \frac{E_{\text{Mo}} - E'_{\text{Fe}}}{4W} \\ & \times \ln \left\{ \frac{[W^2 + (E_{\text{Mo}} - E'_{\text{Fe}})^2/4]^{1/2} + W}{[4W^2/9 + (E_{\text{Mo}} - E'_{\text{Fe}})^2/4]^{1/2} + 2W/3} \right\}. \end{aligned} \quad (7)$$

In Fig. 1 we show the resulting values of  $z$  after minimization of  $E(s, d, t)$  as a function of  $U$  for several values of  $\Delta = E_{\text{Mo}} - E_{\text{Fe}}$ . For sufficiently large values of these quantities,

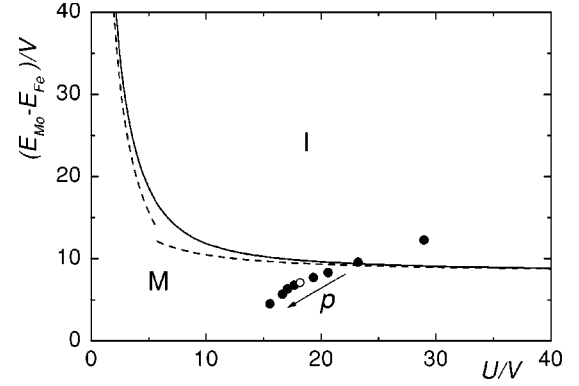


FIG. 2. Phase diagram of the model in the  $E_{\text{Mo}} - E_{\text{Fe}}$  vs  $U$  plane, separating the regions of metallic ( $M$ ) and insulating ( $I$ ) behavior. The dashed lines correspond to the asymptotic analytical expressions (9) for  $U \rightarrow 0$  and  $U \rightarrow \infty$ . The circles correspond to the points listed in Table I. The open circle corresponds to the experimental system at zero pressure. The arrow denotes the direction of increasing pressure.

$z = 0$ . This indicates that the carriers become extremely heavy, the effective bandwidth is zero, and the system is insulating.

For  $z \rightarrow 0$  ( $W \rightarrow 0$ ), the expressions (6) and (7) can be expanded and the minimization problem can be further simplified, allowing a simple analytical description of the metal-insulator boundary. Differentiating the resulting  $E(s, d, t)$  leads to  $t = 0$  and

$$\frac{3(E_{\text{Mo}} - E_{\text{Fe}})}{2\sqrt{38}V} = 2y + (1 + 3y^2)^{1/2} + \frac{1}{(1 + 3y^2)^{1/2}}, \quad (8)$$

$$\frac{9U}{2\sqrt{38}V} = \frac{2}{y} + \frac{3}{(1 + 3y^2)^{1/2}},$$

where  $y = d/(1 - 3m)^{1/2}$ . As  $y$  varies from zero to  $\infty$ , Eqs. (8) map the metal-insulator boundary. Due to the fact that  $t$  goes more rapidly to zero than  $d$  and  $m - 1/3$ , the problem takes a form similar to the metal-insulator transition in the cuprates.<sup>10</sup> Taking the limits of large or small  $y$  in Eqs. (8), asymptotic analytical expressions for the boundary can be derived,

$$E_{\text{Mo}} - E_{\text{Fe}} = \frac{152(2 + \sqrt{3})^2}{27} \frac{V^2}{U}, \quad U \rightarrow 0, \quad (9)$$

$$E_{\text{Mo}} - E_{\text{Fe}} = \frac{4\sqrt{38}}{3} V + \frac{608}{27} \frac{V^2}{U}, \quad U \rightarrow \infty.$$

One can see from here that the insulating behavior due to Coulomb repulsion at Fe sites is not possible if  $E_{\text{Mo}} - E_{\text{Fe}} < (4\sqrt{38}/3)V \approx 8.22V$ , slightly larger than the bandwidth of  $\rho_0$ . This explains the different behavior of the curves in Fig. 1 depending on the value of  $(E_{\text{Mo}} - E_{\text{Fe}})/V$ .

The resulting metal-insulator phase diagram and the asymptotic expressions (9) are represented in Fig. 2. The realization of such a phase transition depends on the possibility of controlling the parameters of the Hamiltonian in

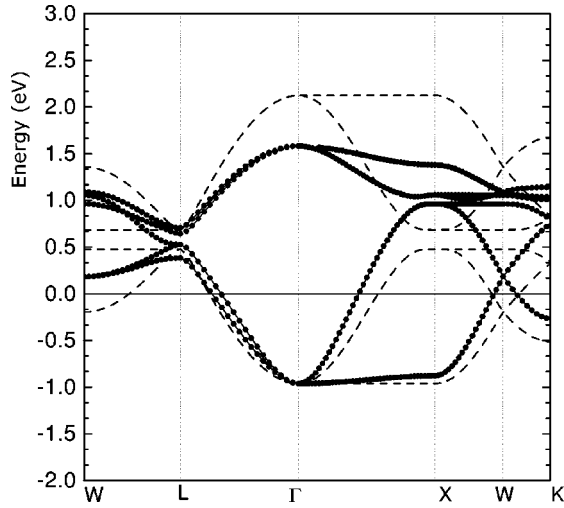


FIG. 3. Calculated  $t_{2g}$  energy bands (full line and solid circles) and fitting using Eq. (1) with  $V'=0$  in the Hartree-Fock approximation (dashed lines). The Fermi energy is at 0 eV. The wave vectors shown are  $W=(\pi/a,0,2\pi/a)$ ,  $L=(\pi/a,\pi/a,\pi/a)$ ,  $\Gamma=(0,0,0)$ ,  $X=(0,0,2\pi/a)$ , and  $K=(3\pi/2a,3\pi/2a,0)$

these materials. As an example, we have studied the effects of pressure (positive or negative) on the parameters for  $\text{Sr}_2\text{FeMoO}_6$ . The Madelung potential at Fe sites should be very different from that at Mo sites due to the large charge difference. In consequence, one expects that the application of pressure or chemical pressure should modify the energy difference between Fe and Mo ( $E_{\text{Mo}} - E_{\text{Fe}}$ ) and also the hybridization parameter  $V$ . These parameters were obtained from a fit of our calculated  $t_{2g}$  energy bands for different values of the lattice parameter to the bands that result from the Hamiltonian (1) with  $V'=0$ , treated in the Hartree-Fock approximation. In particular the band that crosses the Fermi energy was adjusted at its bottom (point  $\Gamma$ ), and  $E_{\text{Mo}} - E_{\text{Fe}}$  was determined from a fit of the bands at the L point. The fit for the experimental lattice parameter is shown in Fig. 3. The

TABLE I. Pressure and parameters of Eq. (1) for different lattice parameters.

$a$ (Å)	$P$ (GPa)	$V$ (eV)	$E_{\text{Mo}} - E_{\text{Fe}}$ (eV)
16.51	-12.47	0.2417	2.967
15.71	-8.37	0.3015	2.886
15.31	-4.57	0.3396	2.824
15.11	-1.69	0.3618	2.789
14.91	1.72	0.3850	2.727
14.81	3.52	0.3964	2.681
14.71	5.36	0.4096	2.577
14.61	7.17	0.4203	2.385
14.51	9.07	0.4494	2.029

bands at higher energies are affected by high-energy states not included in Eq. (1) and a fitting of them is outside our scope. In Table I, we show the resulting parameters and the pressure  $p$  (obtained from the numerical derivative of the total energy in the band-structure calculation with respect to the volume) for different lattice parameters  $a$ . For the experimental  $a = 14.91$  Å at  $p = 0$ , we obtain a small but nonzero  $p$  due to the errors of the method. The corresponding points in parameter space are represented by circles in Fig. 2. One can see that in fact  $\text{Sr}_2\text{FeMoO}_6$  is not far from a metal-insulator transition and this can be achieved by applying a negative pressure estimated as  $-8$  GPa.

In summary, combining band-structure calculations with a slave-boson technique (equivalent to the Gutzwiller approximation<sup>9</sup>) to treat strong correlations, we have studied the possibility of a metal-insulator transition in  $\text{Sr}_2\text{FeMoO}_6$ . We expect that this approach can be used to understand the metallic or insulating behavior in other double perovskites.

We thank G. Zampieri for useful discussions. We were partially supported by CONICET. This work was sponsored by Grant No. PICT 03-06343 of ANPCyT and Grant No. PIP 4952/96 of CONICET.

<sup>1</sup>K.I. Kobayashi, T. Kimura, H. Sawada, K. Terakura, and Y. Tokura, *Nature (London)* **395**, 677 (1998).

<sup>2</sup>A.E. Bocquet, T. Mizokawa, T. Saitoh, H. Namatame, and A. Fujimori, *Phys. Rev. B* **46**, 3771 (1992).

<sup>3</sup>A. Chattopadhyay and A.J. Millis, *Phys. Rev. B* **64**, 024424 (2001).

<sup>4</sup>M.S. Moreno, J.E. Gayone, A. Caneiro, D. Niebieskiwiat, R.D. Sanchez, and G. Zampieri (unpublished).

<sup>5</sup>M.E. Simon, A.A. Aligia, C.D. Batista, E.R. Gagliano, and F. Lema, *Phys. Rev. B* **54**, R3780 (1996).

<sup>6</sup>B. García-Landa, C. Ritter, M.R. Ibarra, J. Blasco, P.A. Algarabel, R. Mahendiran, and J. García, *Solid State Commun.* **110**, 435 (1999).

<sup>7</sup>J. Gopalakrishnan, A. Chattopadhyay, S.B. Ogale, T. Venkatesan, R.L. Greene, A.J. Millis, K. Ramesha, B. Hannoyer, and G. Marrest, *Phys. Rev. B* **62**, 9538 (2000).

<sup>8</sup>M. Itoh, I. Ohta, and Y. Inaguma, *Mater. Sci. Eng., B* **B41**, 55 (1996).

<sup>9</sup>G. Kotliar and A.E. Ruckenstein, *Phys. Rev. Lett.* **57**, 1362 (1986).

<sup>10</sup>C.A. Balseiro, M. Avignon, A.G. Rojo, and B. Alascio, *Phys. Rev. Lett.* **62**, 2624 (1989); **63**, 696(E) (1989).

<sup>11</sup>P. Blaha, K. Schwarz, and J. Luitz, WIEN97, Vienna University of Technology, 1997 [Improved and updated Unix version of the original copyrighted WIEN-code, which was published by P. Blaha, K. Schwarz, P. Soratin, and S.B. Trickey, in *Comput. Phys. Commun.* **59**, 399 (1990)].

<sup>12</sup>D. Singh, *Plane Waves, Pseudopotentials, and the LAPW Method* (Kluwer Academic, New York, 1994).

<sup>13</sup>J.P. Perdew, K. Burke, and M. Ernzerhof, *Phys. Rev. Lett.* **77**, 3865 (1996).

<sup>14</sup>D. Singh, *Phys. Rev. B* **43**, 6388 (1991).

<sup>15</sup>M.E. Simon, A.A. Aligia, and E.R. Gagliano, *Phys. Rev. B* **56**, 5637 (1997), and references therein; H. Rosner, H. Eschrig, R. Hayn, S.-L. Drechsler, and J. Málek, *ibid.* **56**, 3402 (1997), references therein.